

## Differential Charge Polarization of Axial Histidines in Bacterial Reaction Centers Balances the Asymmetry of the Special Pair

A. Alia, Piotr K. Wawrzyniak, Geertje J. Janssen, Francesco Buda, Jörg Matysik, and Huub J. M. de Groot\*

SSNMR, Leiden Institute of Chemistry, Gorlaeus Laboratoria, Einsteinweg 55, P.O. Box 9502, 2300 RA Leiden, The Netherlands

Received April 9, 2009; E-mail: ssnmr@chem.leidenuniv.nl

In photosynthesis, light energy is transformed into chemical energy that sustains most forms of life on earth. The initial process of light-induced electron transfer occurs in photosynthetic reaction centers (RCs). The structures of the RCs of several purple bacteria have been resolved by X-ray diffraction<sup>1</sup> and resemble the photosystem II in higher plants. The RC complex of *Rhodobacter sphaeroides* consists of three polypeptides (H, L, and M) and several cofactors that are arranged in two nearly symmetric branches (Figure 1A). These cofactors include a dimer of excitonically coupled bacteriochlorophyll *a* (BChl *a*) molecules (designated P1 and P2) constituting the primary electron donor (P), two accessory monomeric BChl *a* molecules, two bacteriopheophytin *a* molecules, two ubiquinones, a non-heme iron atom, and a carotenoid molecule. The electronic structure of P is asymmetric in both the ground and excited states, with opposite excess electron densities on P2 in the ground state and P1 in the excited state.<sup>2,3</sup> This affects the electron transfer process and contributes to determining the asymmetric electron flow, which proceeds almost exclusively over the “active” A-branch.<sup>4–6</sup> Stark effect measurements have shown that the electrooptic properties of P\* can be modulated over the width of the extended  $\pi$  system by hydrogen bonding in a donor–acceptor-type push–pull mechanism and that the dipole moment rotates upon excitation.<sup>2</sup>

According to the X-ray structure, bacterial RCs contain four histidines that are coordinated to the  $Mg^{2+}$  of the BChl *a* (also known as axial histidines). His L153 and His M182 interact with accessory BChl's, while His L173 and His M202 interact with the  $Mg^{2+}$  of the special-pair BChl *a* molecules P2 and P1, respectively, with their  $\pi$  nitrogens within hydrogen-bonding distance of a water molecule.<sup>1</sup> We selectively probed the environment of P and accessory BChl's in bacterial RCs from *R. sphaeroides* grown in the presence of  $\tau$ -<sup>15</sup>N- or uniformly [<sup>13</sup>C, <sup>15</sup>N]-labeled His and resolved a ground-state mechanism that is complementary to the push–pull tuning, involving one of the axial histidines. One-dimensional cross-polarization–magic-angle-spinning (CP–MAS) <sup>15</sup>N NMR spectra of RCs in which the histidines are labeled at both the  $\tau$  and  $\pi$  nitrogens or only at the  $\tau$  nitrogen of the imidazole ring are presented in Figure 1C,D. The assignment of the <sup>15</sup>N resonances of the imidazole ring of the histidines in the two spectra is summarized in the table within Figure 1. The signal at 225 ppm is assigned to the imidazole  $\tau$  nitrogen of histidines that are coordinated to a  $Mg^{2+}$  in a BChl ring. This assignment is based on the recent complete <sup>1</sup>H, <sup>13</sup>C, and <sup>15</sup>N assignment of imidazole side-chain resonances of the histidines in the LH2 complex detected with MAS NMR.<sup>7</sup> Another weak signal from the  $\tau$  nitrogen of  $Mg^{2+}$ -coordinated histidines is visible at 220 ppm. The difference in the peak intensities at 225 and 220 ppm extracted from the spectra by Lorentz curve-fitting (data not shown) indicates that three of the four histidines resonate at 225 ppm, while the fourth resonates at 220 ppm. The ring-current effect cannot explain the dispersion of the  $\tau$ -nitrogen signals, since all of the axial histidines should

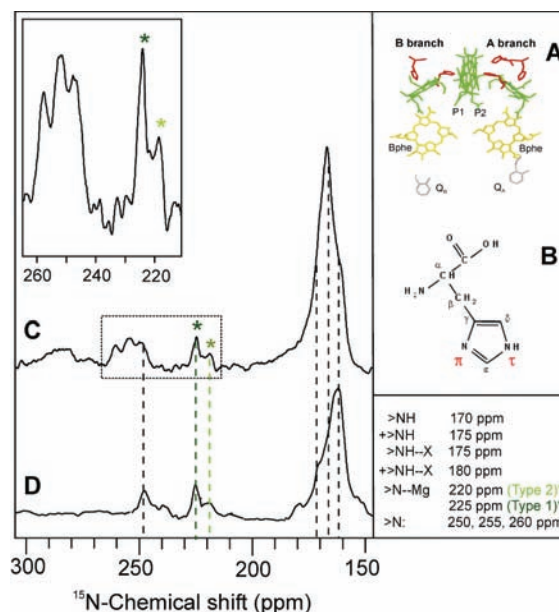


**Figure 1.** (A) Arrangement of cofactors in RCs of *R. sphaeroides* (R26). (B) Structure of His with nomenclature. (C, D) CP–MAS <sup>15</sup>N NMR spectra of (C) uniformly and (D)  $\tau$ -<sup>15</sup>N-His-labeled RCs measured in a magnetic field of 17.6 T at 220 K with a spinning frequency of 12 kHz. The data were collected in  $\sim 15\,000$  scans with an acquisition time of 20 ms and a recycle time of 1 s. A detailed view of the region between 205 and 265 ppm is shown in the inset (upper left). Assignment of the <sup>15</sup>N peaks obtained from C and D is shown at the lower right. The asterisks indicate the positions of center-band signals from  $\tau$  nitrogens of axial histidines that interact with BChl *a* in the RC. The spectra reveal two different types of axial histidines, designated type 1 (dark-green dashed lines) and type 2 (light-green dashed lines), in bacterial RCs.

experience similar ring-current effects as a result of the similar distances ( $\sim 2.11$ – $2.35$  Å) between their  $\tau$  nitrogens and the  $Mg^{2+}$  of coordinated BChl<sup>8</sup> [see the Supporting Information (SI)]. Recently, solid-state photo-CIDNP <sup>13</sup>C NMR studies have shown that the BChl of the special pair in the active branch, P2, has a significantly different ground-state electronic structure than P1 and the accessory BChl's.<sup>3,9</sup> In line with these results, we attribute the signal at 220 ppm (type-2 His) to the axial His coordinated to P2.

To gain further insight into the electronic structure and charge states of axial histidines, we performed <sup>1</sup>H–<sup>13</sup>C heteronuclear dipolar correlation studies. Figure 2 shows a 2D <sup>1</sup>H–<sup>13</sup>C dipolar correlation spectrum of [<sup>13</sup>C<sub>6</sub>, <sup>15</sup>N<sub>3</sub>]-His-labeled RCs. The correlation signals from the axial histidines at <sup>1</sup>H chemical shifts of  $\sim 2$  ppm are well-separated from the response of the other histidines at 5–8.5 ppm. The upfield shift of the  $\delta$ - and  $\epsilon$ -<sup>1</sup>H signals for the axial histidines relative to the other histidines in the RC reflects the ring-current shift effect experienced by nuclei in close proximity to the conjugated porphyrin ring system of BChl. Interestingly,  $\delta$  and  $\epsilon$  protons of the axial histidines appear at two distinct positions in both the <sup>1</sup>H and <sup>13</sup>C

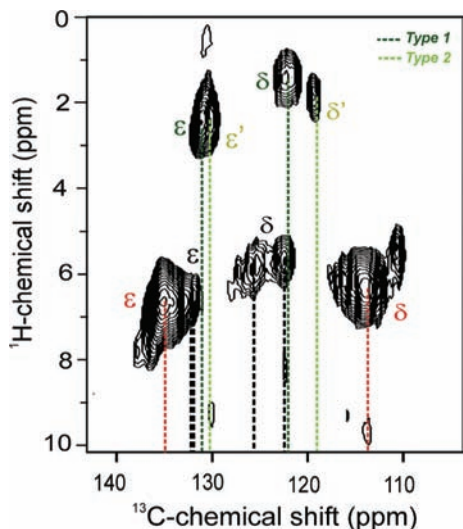


**Figure 2.** Contour plot sections of a 2D  $^1\text{H}$ – $^{13}\text{C}$  heteronuclear dipolar correlation spectrum of [ $^{13}\text{C}$ , $^{15}\text{N}$ ]-His-labeled bacterial RCs of *R. sphaeroides* collected at a magnetic field strength of 17.6 T. The cross-peaks from  $^1\text{H}$  and  $^{13}\text{C}$  at the  $\delta$  and  $\epsilon$  positions of axial histidines are shown in green. The significant ring-current effects on the axial histidines caused separation of their cross-peaks from those of nonaxial histidines in the RC. Two types of axial histidines, type 1 (dark-green) and type 2 (light-green) were detected.

dimensions (Figure 2), revealing two different types of axial histidines. Integration of the  $^1\text{H}$ – $^{13}\text{C}$  cross-peaks shows that one axial His is different from the other three. These results are in accordance with the  $^{15}\text{N}$  resonance data shown in Figure 1 and validate the observation of an axial His with a distinctly different electronic structure in the bacterial RC. Density functional theory (DFT) calculations performed on BChl–His complexes with axially coordinated histidines (see the SI) indicated that axial histidines are neutral and that local strain in the tightly folded protein can cause strong H-bonding of the  $\pi$  nitrogen and differences in the chemical shifts of the  $\tau$  nitrogen and the  $\delta$  and  $\epsilon$  carbons (Table 1 in the SI). The calculated electrostatic potential charges indicate a partial positive charge of +0.19 on the imidazole ring of this special axial His, which can be compared with the charge of +0.10 on the imidazole ring of an axial His that is not involved in H-bonding at its  $\pi$  nitrogen (Figure 3). NMR data and modeling thus provide converging evidence that the electronic structure of one of the axial histidines, most likely His L173, is different from the other three and balances excess negative charge on P2 with twice the amount of positive charge as on the other axial histidines, which is stabilized by a strong hydrogen bonding environment at the  $\pi$  nitrogen. Since it operates perpendicular to the push–pull mechanism, it could explain why the dipole moment rotates upon excitation.<sup>2</sup>

According to the X-ray structure, bacterial RCs contain a total of 20 histidines. Among the 16 nonaxial histidines, four (His L190, His L230, His M219, and His M266) are located in the vicinity of the paramagnetic  $\text{Fe}^{2+}$ , where His L190 and His M219 are H-bonded to  $\text{Q}_\text{A}$  and  $\text{Q}_\text{B}$ , respectively.<sup>1,10</sup> It is very unlikely that the histidines close to the Fe are detected in the 2D data in Figure 2. This is corroborated by  $T_1$  relaxation measurements, which show that the  $T_1$  relaxation times of the various cross-peaks are quite similar (data not shown). Comparison of the  $^{13}\text{C}$  chemical shifts of the imidazole rings of nonaxial histidines in the RC with the side-chain response of neutral and cationic histidines in model systems<sup>7</sup> shows that a large number of nonaxial histidines are neutral species with the  $\delta$  and  $\epsilon$  carbons resonating at 113.6 and 134.9 ppm respectively, while a few carry a positive charge on their imidazole

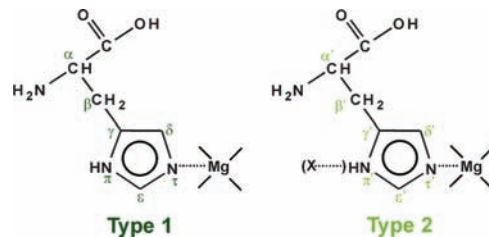


**Figure 3.** Schematic representation of DFT models of the type-1 and type-2 BChl–His neutral complexes without and with H-bonding at the  $\pi$  nitrogen, respectively. The total imidazole ring charge of the type-1 and type-2 histidines are calculated to be +0.10 and +0.19, respectively. The  $\tau$ -nitrogen–Mg distance is shortened by 0.03 Å in the presence of the H-bond at the  $\pi$  nitrogen.

ring, with unique carbon shifts of 132.5 ppm for  $\epsilon$  and 122.2 or 125.7 ppm for  $\delta$ . DFT calculations suggest that the  $\delta$   $^{13}\text{C}$ 's of positively charged histidines resonate with shifts of  $\sim 123$  ppm.<sup>11</sup> However, a downfield shift of  $\sim 2.5$  ppm is observed for the  $\delta$  carbon when both the  $\tau$  and  $\pi$  nitrogens of the cationic His are involved in H-bonding interactions. From these data, it can be inferred that one or more nonaxial histidines in bacterial RCs have both nitrogens of the imidazole ring fully protonated and involved in H-bonding interactions.

In summary,  $^{15}\text{N}$  and  $^{13}\text{C}$  NMR data and DFT calculations have revealed an asymmetric electronic environment of P, since one axial His, most probably L173, has excess positive charge. L173 is coordinated to P2 and is protonated and H-bonded to a water molecule. The special His may have a significant impact on the electric dipole moment in the ground state and its change in magnitude and angle upon excitation and also may lower the barrier for bidirectional proton-coupled electron transfer, thereby facilitating thermodynamic control of proton transfer over the rate and direction of electron transfer.<sup>12</sup>

**Acknowledgment.** This work was supported by the EU and The Netherlands Organization for Scientific Research (NWO) through a TOP Grant (to H.J.M.d.G.) and a VIDI Grant (to J.M.). The use of supercomputer facilities was sponsored by the Stichting Nationale Computerfaciliteiten (NCF) with support from the NWO.

**Supporting Information Available:** Materials and Methods and DFT results. This material is available free of charge via the Internet at <http://pubs.acs.org>.

## References

- (1) Ermler, U.; Michel, H.; Schiffer, M. *J. Bioenerg. Biomembr.* **1994**, *26*, 5.
- (2) Moore, L. J.; Zhou, H.; Boxer, S. G. *Biochemistry* **1999**, *38*, 11949.
- (3) Schulten, E. A. M.; Matysik, J.; Alia, K.; Kihne, S.; Raap, J.; Lugtenburg, J.; Gast, P.; Hoff, A. J.; de Groot, H. J. M. *Biochemistry* **2002**, *41*, 8708.
- (4) Allen, J. P.; Cordova, J. M.; Jolley, C. C.; Murray, T. A.; Schneider, J. W.; Woodbury, N. W.; Williams, J. C.; Niklas, J.; Klihm, G.; Reus, M.; Lubitz, W. *J. Photosynth. Res.* **2009**, *99*, 1.
- (5) Lee, H.; Cheng, Y.-C.; Fleming, G. R. *Science* **2007**, *316*, 1462.
- (6) Wang, H.; Lin, S.; Allen, J. P.; Williams, J. C.; Blankert, S.; Laser, C.; Woodbury, N. W. *Science* **2007**, *316*, 747.
- (7) Alia, Matysik, J.; Soede-Huijbregts, C.; Baldus, M.; Raap, J.; Lugtenburg, J.; Gast, P.; van Gorkom, H. J.; Hoff, A. J.; de Groot, H. J. M. *J. Am. Chem. Soc.* **2001**, *123*, 4803.
- (8) Roszak, A. W.; Gardiner, A. T.; Isaacs, N. W.; Cogdell, R. J. *Biochemistry* **2007**, *46*, 2909.
- (9) Prakash, S.; Alia, Gast, P.; de Groot, H. J. M.; Jeschke, G. and; Matysik, J. *Biochemistry* **2007**, *46*, 8953. Daviso, E. Ph.D. Thesis, Leiden University, The Netherlands, 2008.
- (10) Remy, A.; Gerwert, K. *Nat. Struct. Biol.* **2003**, *10*, 637.
- (11) Wawrzyniak, P. K.; Alia, A.; Schaap, R. G.; Heemskerk, M. M.; de Groot, H. J. M.; Buda, F. *Phys. Chem. Chem. Phys.* **2008**, *10*, 6971.
- (12) Hodgkiss, J. M.; Rosenthal, J.; Nocera, D. G. In *Handbook of Hydrogen Transfer*; Schowen, R. L.; Klinman, J. P.; Hynes, J. T.; Limbach, H.-H., Eds.; Wiley-VCH: Weinheim, Germany, 2006.

JA9028507